Poly(L-lactic acid) with Segmented Perfluoropolyether Enchainment

Dahlia Haynes,[†] Amit K. Naskar,[†] Akhilesh Singh,[‡] Chih-Chao Yang,[§] Karen J. Burg,[§] Michael Drews,[‡] Graham Harrison,[||] and Dennis W. Smith, Jr.*[,†]

Department of Chemistry, School of Material Science and Engineering, Department of Bioengineering, and Department of Chemical and Biomolecular Engineering, Center for Advanced Engineering Fibers and Films, Clemson University, Clemson, South Carolina 29634

Received May 31, 2007; Revised Manuscript Received October 12, 2007

ABSTRACT: A novel approach to property enhancement of poly(L-lactic acid) (PLLA) through the use of perfluoropolyether (PFPE) enchainment is described. Segmented copolymers (FluoroPLA) exhibit tailored surface properties with reasonably high molecular weights and low polydispersities compared to PLLA alone using standard ring-opening polymerization procedures in the presence of tin catalysts. Low loadings of PFPE content (ca. 1−5 wt %) decreases surface energies compared to PLLA from 35 to 38 to 15−18 mN/m^2, similar to values reported for poly(tetrafluoroethylene). Ultimate strain studies of FluoroPLA fibers and films have shown a dramatic increase (>300% elongation) over PLLA. This new class of polymer may further expand the use of renewable resources in a variety of applications such as flame retardants, chemical resistant fibers and/or fabrics with tailorable surface energies and wetting properties.

Introduction

A monumental shift in the transition from petroleum-based resources to more sustainable plant-based technologies is now viewed by many as a necessity for the continuation of our current population and economic growth.[1,2] The idea of "renewable resources", which is defined in one way as "any resource that can be replenished through biomass production such as wheat, corn, and starch"[3] is now much more promising due to global market and environmental demands. Poly(L-lactic acid) (PLLA) is a commercial thermoplastic polyester prepared by the ring-opening polymerization of corn-derived L-lactide.[4] On the basis of many of its favorable properties and cost, semicrystalline PLLA offers the highest potential of any renewable polymer and currently challenges some markets dominated by petroleum-derived plastics such as polyethylene, poly(ethylene terephthlate), and polystyrene.[5−9] PLLA, however, is limited from many fiber, film, and textile applications due to its unfavorably placed glass transition temperature (T_g), its loss of mechanical properties at high processing temperatures, and its hydrolytic instability.

Researchers throughout the world are engaged to modify and overcome limitations associated with PLLA. Many approaches such as copolymerization,[10−12] blending[13,14] and stereopolymerization[15] have been reported to altar the properties of PLLA and increase or facilitate its market entry into a variety of applications. Our current research involves the discovery of new strategies to improve the properties of renewable materials for broad impact in non-conventional applications and hopeful renewable feedstock price reduction.

Here, we report a simple route to the first segmented PLLA based material using commercial perfluoropolyether diols as macroinitiators for the ring-opening polymerization (ROP) of L-lactide. This procedure produces novel ABA triblock copolymers with greatly enhanced properties with minimum fluorination (see Scheme 1a). The new copolymers exhibit improved melt processability, greater surface hydrophobicity, increased ductility and elongation, and controlled environmental stability over PLLA homopolymer. The polymerization is initiated with stannous octoate and allows for high molecular weight polymers with relatively low polydispersities. Varying the amount of perfluoropolyether allows for tailorable characteristics including surface energies, wettability, and enhanced thermal and mechanical properties.

* Correspondence should be addressed to this author. E-mail: dwsmith@clemson.edu.
[†] Department of Chemistry, Clemson University.
[‡] School of Material Science and Engineering, Clemson University.
[§] Department of Bioengineering, Clemson University.
[||] Department of Chemical and Biomolecular Engineering, Center for Advanced Engineering Fibers and Films, Clemson University.

Experimental Section

Materials. L-Lactide, stannous octoate, and chloroform-*d* were purchased from Aldrich, and poly(tetrafluoroethylene oxide-*co*-difluoromethylene oxide) α,ω-diol (Fomblins Z DOL) was obtained from Solvay-Solexis. All other chemicals and reagents were purchased from Fisher or Sigma Aldrich and used as received unless otherwise stated.

Instrumentation. ^{1}H, ^{13}C, and ^{19}F NMR spectra were obtained using the Bruker AF-300 spectrometer system. Chloroform-*d* was used as solvent and chemical shifts reported were internally referenced to tetramethylsilane (0 ppm), and $CDCl_3$ (77 ppm) for ^{1}H and ^{13}C nuclei, respectively. Gel permeation chromatography (GPC) data was collected in $CHCl_3$ using a Waters Alliance refractive index detection at 35 °C and equipped with Polymer Labs PLGel 5 mm Mixed-C and Mixed E columns. Retention times were calibrated against Polymer Labs Easical PS-2 polystyrene standards. Thermal gravimetrical analysis (TGA) data were obtained from a Mettler-Toledo 851 TGA/SDTA System at a heating rate of 5 °C/min in a nitrogen atmosphere. Differential scanning calorimetry (DSC) was obtained from TA Instruments Q1000 system with an auto sampler and liquid nitrogen cooling system. Analysis was carried out using TA Instruments Universal Analysis Software. Heating and cooling ramp rates for all samples were carried out from −120 to +190 °C at 10 °C/min followed by isothermal heating for 5 min at 190 °C. The glass transition (T_g) was obtained from a second heating curve after cooling at 10 °C /min. The reported T_g value was taken at the midpoint of the C_p curve.

Rheology. Viscoelastic measurements were performed using a Rheometric Scientific ARES rheometer. Samples were tested using a cone and plate geometry with a diameter of 25 mm where dynamic strain and frequency tests were conducted at a temperature of 165 °C.

10.1021/ma0712192 CCC: $37.00
Published on Web 12/04/2007

Scheme 1. Schematic Illustration of L-lactide Ring Opening Polymerization (ROP) with and without PFPE Macroinitiator and Illustration of Resulting Surface Effects (a) and Synthetic Reaction Schematic of FluoroPLA Copolymer (b)

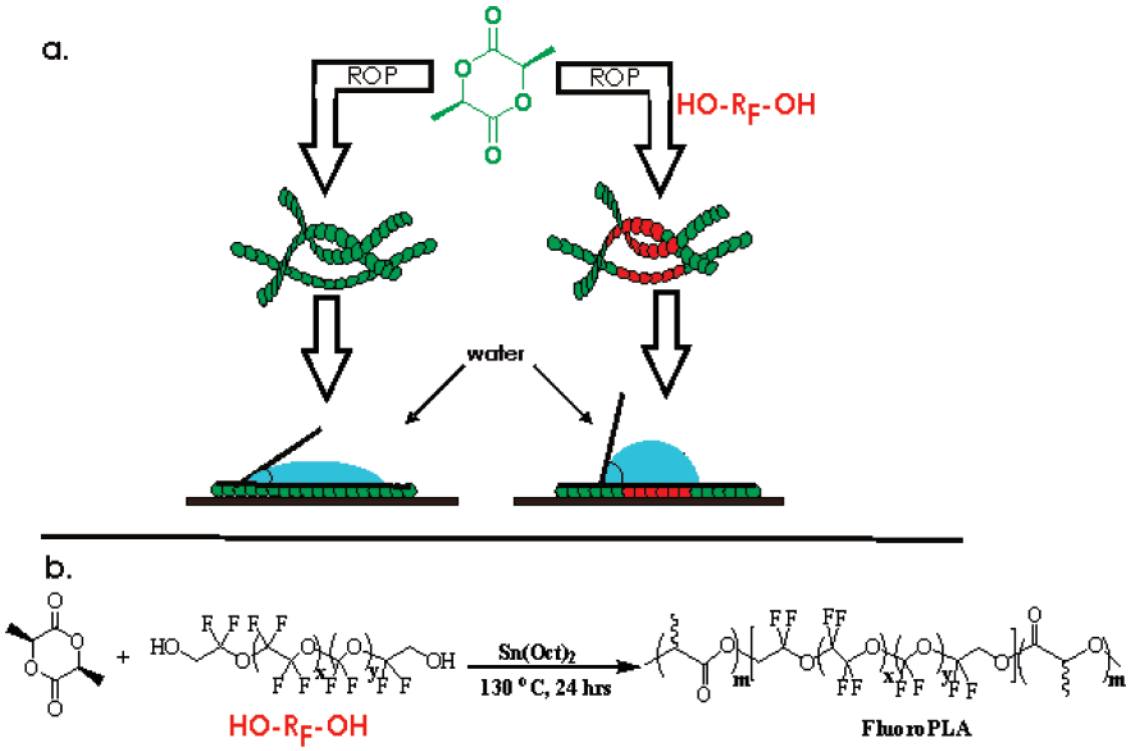

FTIR Analysis. Fourier transform infrared (FTIR) spectroscopy was performed on thin films of PLLA and copolymers and the neat liquid of PFPE using a ThermoNicolet Magna-IR 550 FTIR spectrometer equipped with a Nic-Plan microscope, with a resolution of 2 cm^{-1} using 16 scans. Solutions of polymers in $CHCl_3$ were drop cast on KRS-5 plates under a heat lamp. Estimated film thickness was <1 μm.

Contact Angle Measurements. Static water contact angle measurements were obtained with a Kruss G10 instrument and the average static contact angles were obtained using at least six droplets on each film specimen. The static contact angle (equilibrium) were measured using a Krüss Contact Angle machine by sessile drop method for water, glycerol, formamide, methylene iodide, and *n*-hexadecane on PLLA and high molecular weights of the PLLA−PFPE copolymers dip coated on silicone wafers.

AFM. Atomic force microscopy was performed on nonoriented spin-coated films of PLLA and FluoroPLA20 copolymers using a Digital Instrument Multimode Nanoscope (IV) system in tapping mode using silicon cantilever tips with scan rates between 0.5 and 1 Hz.

Blend Preparation of 1—20 wt % PFPE Content in Blend. Solution blending took place in $CHCl_3$ as the desired solvent obtaining the 1, 5, 10, and 20 wt % compositions of PFPE and PLLA. The milky PFPE/PLLA blend suspensions were precipitated in swirling methanol and dried in vacuo.

Film Preparation for Contact Angle Measurements. Films of PLLA, 1, 5, 10, and 20 wt % FluoroPLA copolymer and blend was made using 10% solvent to polymer ratio, The solutions were then spun cast onto glass plates or silicon wafers and air-dried slowly for 72 h and then placed in a vacuum oven for further solvent removal.

Degradation Studies of Polymer Film Samples. Polymer films were cast from a 10% (w/v) solution in $CHCl_3$ using Teflon sheets. After 72 h of drying at a temperature of 4 °C, the samples were recovered and disks with a diameter of 17 mm were punched from the film sheets using a cork bore. The film disks were then placed in vacuo at room temperature until constant weights were achieved. To determine the in vitro degradation profiles, weighed films were placed in 10 mL of phosphate buffered saline (PBS, pH 7.4, 0.15 M) and kept at 37 °C in an incubator with constant agitation. Samples were removed at designated times, blotted with kimwipes and freeze-dried using a lyophilizer at −35 °C for approximately 72 h. Polymer mass loss was calculated from the following formula: mass loss (%) = 100 − (mass (dry) × 100/(original mass)).

General Procedure of the Synthesis of ABA Triblock Copolymer. To a 5 mL glass ampule under nitrogen were added the desired composition amounts of poly(tetrafluoroethylene oxide-*co*-difluoromethylene oxide) α,ω-diol, Fomblins Z-Dol (PFPE), L-LA, and $Sn(Oct)_2$ (100 μL of 0.01 mol L^{-1} solution in anhydrous toluene). The ampule was then heated to facilitate mixing and sealed under vacuum. The tube was then immersed in a preheated oil bath at 130 °C for 24 h. The crude product was then dissolved in chloroform and precipitated into cold swirling methanol repeatedly. The resulting polymer was dried in vacuo to afford a white fibrous material. Yield: >90%. FTIR (neat film) (cm^{-1}): 693, 754, 869, 918, 956, 1044, 1080, 1183, 1127, 1180, 1264, 1359, 1382, 1453, 1684, 1749, 2881, 2945, 2996. ^{1}H NMR (300 MHz, $CDCl_3$), δ (ppm): 5.14 (q, $J = 7.30$ Hz, α-H, PLLA), 4.56 (q, $J = 9.96$ Hz, $-CF_2CF_2OCH_2-$, PFPE) 4.34 (q, $J = 6.85$ Hz, $-CF_2OCH_2-$, PFPE) 1.56 (d, $J = 6.88$ Hz, $-CH_3$, PLLA). ^{13}C NMR (300 MHz, $CDCl_3$), δ (ppm): 169.70, 129.11, 128.31, 125.38, multiplet 118.43−114.23, 16.72. ^{19}F NMR (300 MHz, $CDCl_3$), δ (ppm): −51.7, −53.4, −55.1, −56.7, −77.4, −79.52, −82.8, −85.1, −88.8, −90.5, −92.1, −127.27, −130.83. See Table 1 for other characterization details.

Results and Discussion

In this study, commercially available hydroxyl-terminated perfluoropolyethers (PFPE) of different molecular weights (Fomblin Z dols, donated by Solvay Solexis, S.p.A.) were used as macroinitiators in the ring-opening polymerization (ROP) of L-lactide. Perfluoropolyether (PFPE) polymers offer an array of advantageous properties such as low surface energy, good oxidative stability, solvent and high-temperature resistance.[16] Previous studies incorporating PFPE segments in polyesters[17] and other fluorinated additives[18,19] have been shown to improve intrinsic properties. Copolymers of 1, 5, 10, and 20 wt % PFPE

Table 1. Selected Physical Characteristics of Polymers

sample	PFPE feed, wt % (exptl)[a]	M_n[b] × 10^{-3}	M_w/M_n[b]	T_m[c]	T_c[c]	T_g[c]	% cryst[d]	T_d[e]
PFPE	100 (100)	0.5	1.1			−104		270
PLLA		57	2.1	176	111	61	51	253
FluoroPLA1	1 (0.95)	58	1.8	173	96	54	53	245
1% PFPE blend	1 (0.99)	58	2.7	175	109	59	51	243
FluoroPLA5	5 (4.8)	64	1.7	166	92	51	44	246
5% PFPE blend	5 (5)	57	2.8	174	102	58,[g] −101[f]	23	253
FluoroPLA10	10 (8.3)	51	1.9	174	104	59	37	251
10% PFPE blend	10 (9.7)	59	3.3	175	92	59,[g] −101[f]	46	265
FluoroPLA20	20 (17.2)	42	1.8	161	62	45	31	239
20% PFPE blend	20 (19)	60	3.6	175	92	60,[g] −99[f]	52	273

[a] Calculated from ^{19}F NMR. [b] Determined by GPC. [c] Determined by DSC. [d] Determined from fully crystalline PLLA and DSC. [f] Determined by TGA. [e] Determined by TGA. [g] Transition associated with PLLA. [f] Peak associated with PFPE.

segments (FluoroPLA1−20) were incorporated using PFPEs of molecular weights (M_n) 1472 and 3561 determined by NMR analysis. The schematic of the reaction is shown in Scheme 1b.

FTIR analysis of the copolymers show the absence of the broad OH stretch at 3360 cm^{-1} present in homo PFPE and the PFPE/PLLA blends. Monomer conversion and growth of polymer was determined by NMR analysis of the $-CH_2-$ region for the perfluoropolyether and the $-CH_3$ region for the PLLA segments. Parts a−c of Figure 1 describe ^{1}H, ^{19}F, and ^{13}C NMR spectra of the resulting FluoroPLA copolymer. The ^{1}H NMR spectrum of PFPE starting material is characterized by the multiplet at 3.5 ppm assigned to the $-CH_2-$ signals of the perfluoropolyether segment and the hydroxyl proton signal at 5.2 ppm in the starting perfluoropolyether diol. The hydroxyl proton signal is not visible in the FluoroPLA copolymers as expected. The shift of the $-CF_2CH_2O-$ multiplet signals to 4.4 ppm from the original signals at 3.5 ppm shows the effect of the new ester linkage. The signals corresponding to PLLA are a doublet at 1.56 ppm and a quartet at 5.1 ppm for the $-CH_3-$ and $-CH-$ groups, respectively. The ^{19}F NMR spectra is similar to the perfluoropolyether precursor, except for the new signals for the $-CF_2CH_2OR-$ (R = PLLA units) segments at −77.4 and −79.5 ppm compared to the starting $-CF_2CH_2OH$ end group signals at −85.1 and −82.8 ppm. Minor signals from the unreacted perfluoropolyether end groups are slightly visible and integration allows for the determination of PFPE wt % incorporation.[17−18]

The molecular weight of copolymers was determined by gel permeation chromatography (GPC). Relatively high molecular weights (M_n = 40−65K) were obtained with low polydispersities. GPC analysis in Figure 2 shows a distinct peak for the FluoroPLA20 copolymer that is different from that for PLLA, PFPE and the corresponding blend. The negative, inverted signal for the PFPE is due to the disparity of refractive indices between the solvent and the fluorinated oligomer. The formation of the ABA block copolymer is rationalized by the overlap of the positive and negative curves (cf. Figure 2b), whereas compared to the blend, the negative and positive curves corresponding to the PLLA and PFPE signals are eluted at different times as shown in Figure 2d.

Photographs of the new copolymers in comparison to isocomponent blends show distinct differences in optical clarity (cf. Figure 8). In contrast to a 5−20 wt % blend of PFPE in PLLA where macrophase separation of PFPE and PLLA segments is obvious due to the opacity of the spun cast film, the FluoroPLA 5−20 copolymers are processed into clear tough plastic films (Figure 8).

Glass transition temperatures (T_g by DSC) decreased with the increase in perfluoropolyether content (Figure 3). With 20 wt % loading of PFPE, the T_g is lowered by 15−20 °C from

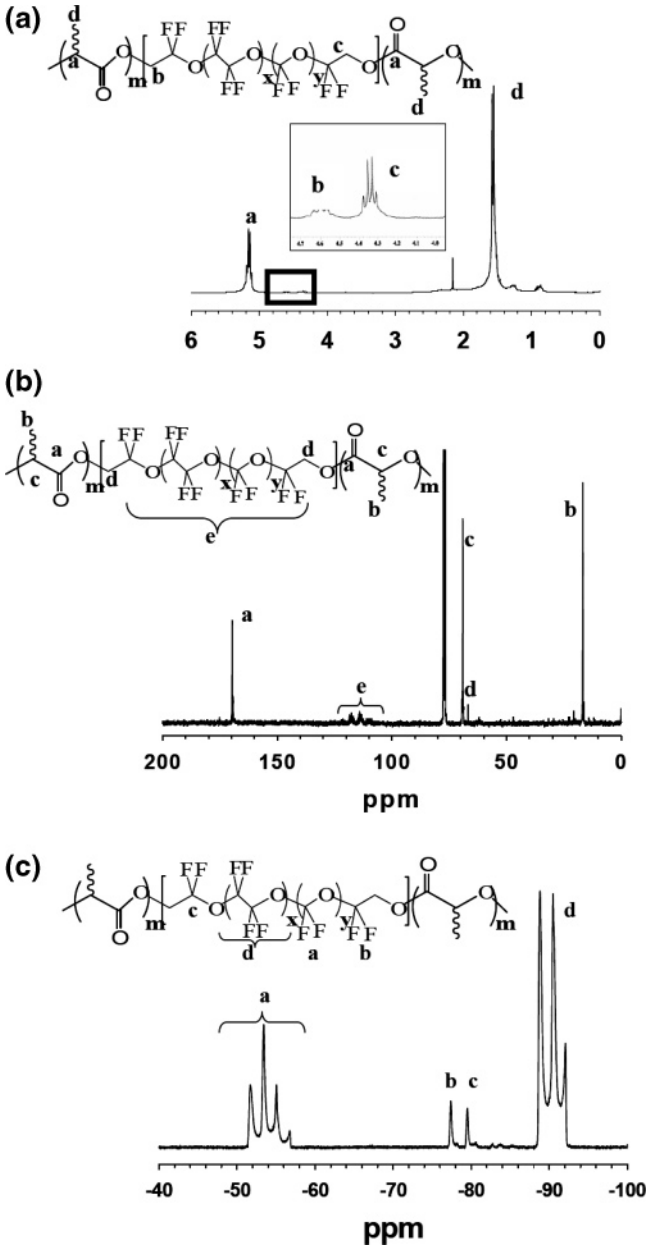

Figure 1. (a) ^{1}H NMR spectrum of FluoroPLA20. (b) ^{13}C NMR spectrum of FluoroPLA20. (c) ^{19}F NMR spectra of FluoroPLA20.

that of the PLLA homopolymer. The changes in glass transitions can be attributed to the effect of PFPE content on the heat capacity and expansion coefficient. Dense chain packing of the crystalline regions of PLLA is further interrupted by the elastomeric PFPE segments which affect volume and enthalpy variations associated with glass transitions. These transforma-

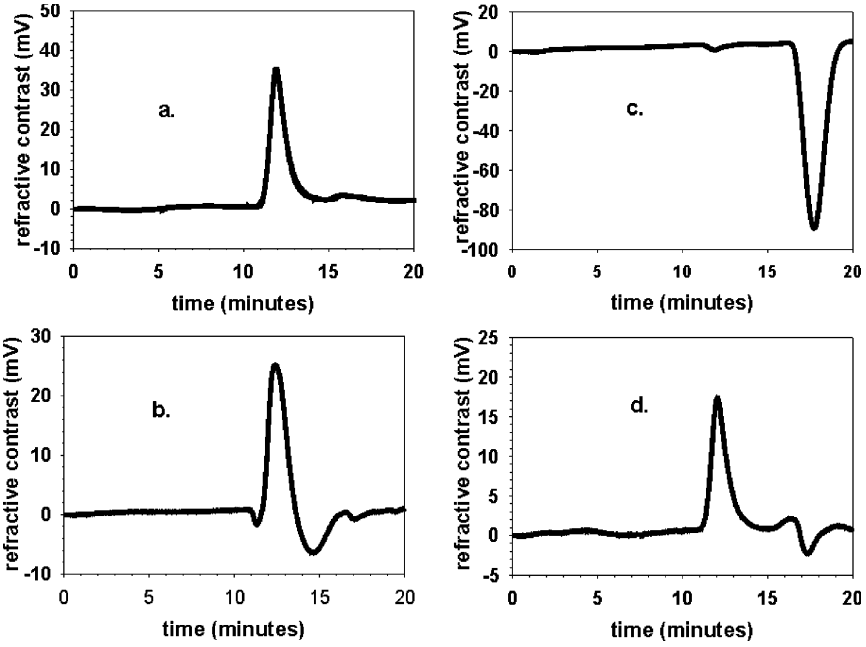

Figure 2. GPC Chromatograms of (a) PLLA, (b) PFPE, (c) FluoroPLA20, and (d) 20 wt % PFPE.

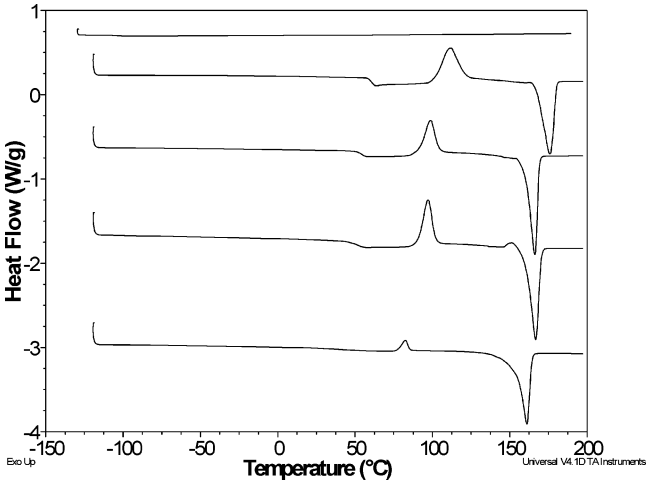

Figure 3. DSC thermograms of (a) PFPE, (b) PLLA, (c) FluoroPLA5, (d) FluoroPLA10, and (e) FluoroPLA20.

tions offer rationale into the dramatic changes in mechanical properties (cf. Figure 6) when a load is applied. In general, other DSC changes due to the inclusion of PFPE into PLLA include decreased crystallization temperature, melting temperature and overall crystallinity at high loading of PFPE. Selected property characteristics are shown in Table 1.

Addition of fluorinated additives and in particular cross-linked PFPEs have been known to dramatically lower surface energies.[20] Contact angle measurements were performed using a variety of polar and nonpolar liquids as shown in Figure 4a and the surface energy of PLLA and FluoroPLA copolymers were calculated by the Owens, Wendt, Rabel, and Kaelble method, which assumes that the total surface energy is the sum of its polar and dispersive components.[21,22] The solvent wettability results and surface energies using the Kaelble method are summarized in Figure 4b.

The surface energy of PLLA was found to be in close proximity with literature values of 35−43 mN/m.[23] Incorporation of PFPE, as low as 1 wt % of the PLLA segments, lowered the polar and dispersive components of PLLA from 8 and 27 mN/m to 2 and 15 mN/m, respectively (see Supporting Information).

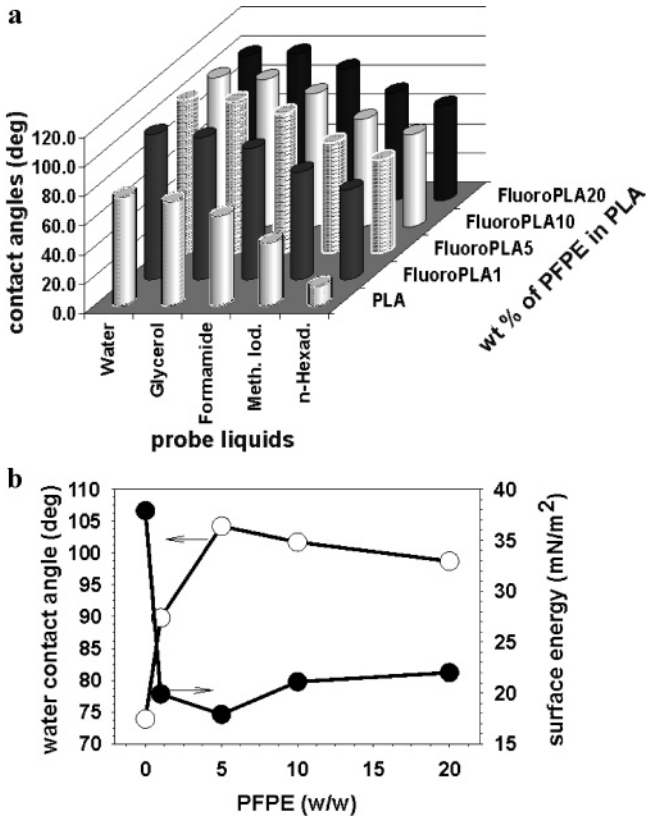

Figure 4. (a) Contact angles of copolymer films in various liquids and (b) summarized trend detailing surface energy and water contact angles for PLLA and FluoroPLA copolymers.

Further incorporation of PFPE segments did not alter the surface energies significantly yet increased the copolymer (≥5 wt %) hydrophobicity (water contacts angle ≥100 ± 0.8 °). FluoroPLA copolymers showed surface energies very similar to polytetrafluoroethylene (PTFE) which is reported to be 18−20 mN/m.[24]

Surface morphological characterization of PLLA and FluoroPLA copolymer films were investigated by atomic force microscopy (AFM). Height and phase images with a variation

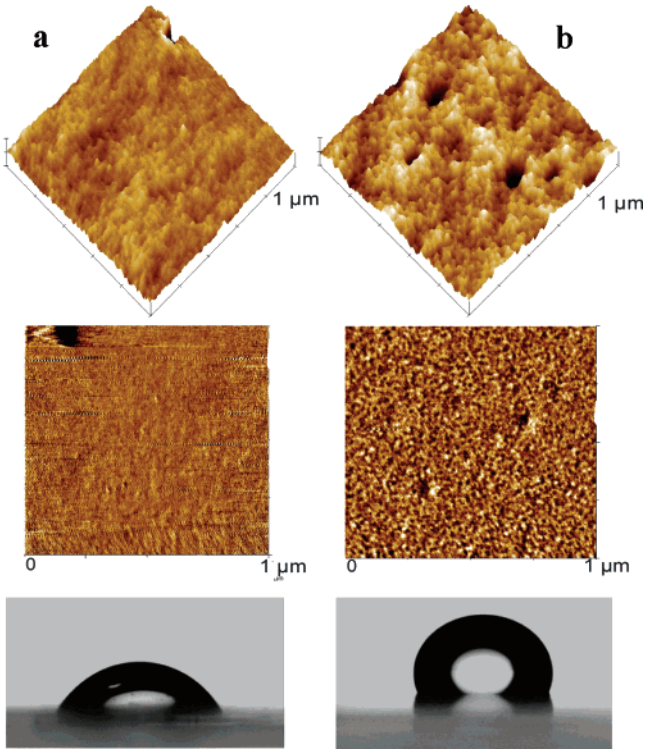

Figure 5. Atomic force microscope topology and phase studies on 1 × 1 μm images of (a) PLLA and (b) FluoroPLA20 polymers and sessile water drop images on spun cast films.

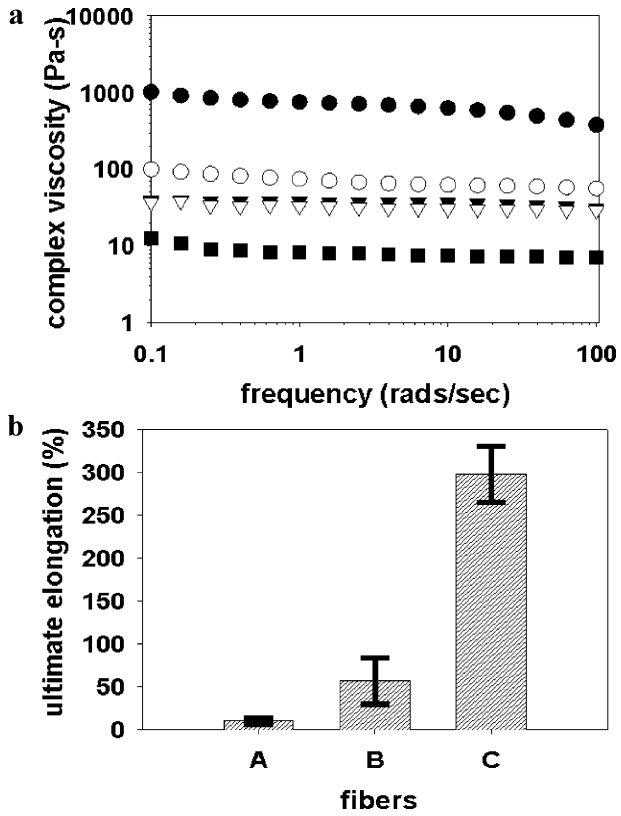

Figure 6. (a). Complex viscosity vs frequency at 165 °C for PLLA (-●-), FluoroPLA1 (-○-), FluoroPLA5(-▼-), FluoroPLA10 (-▽-), and FluoroPLA20 (-■-) copolymers and (b) ultimate tensile elongation of (A) PLLA, (B) FluoroPLA5 (4.0 K), and (C) FluororPLLA5 (2.0 K) copolymer fibers.

of 20 wt % of PFPE content in the PLLA matrix (cf. Figure 5) illustrate the effect of fluorine content on nanoscale morphology. In the topographical mode, surface height is altered from neat

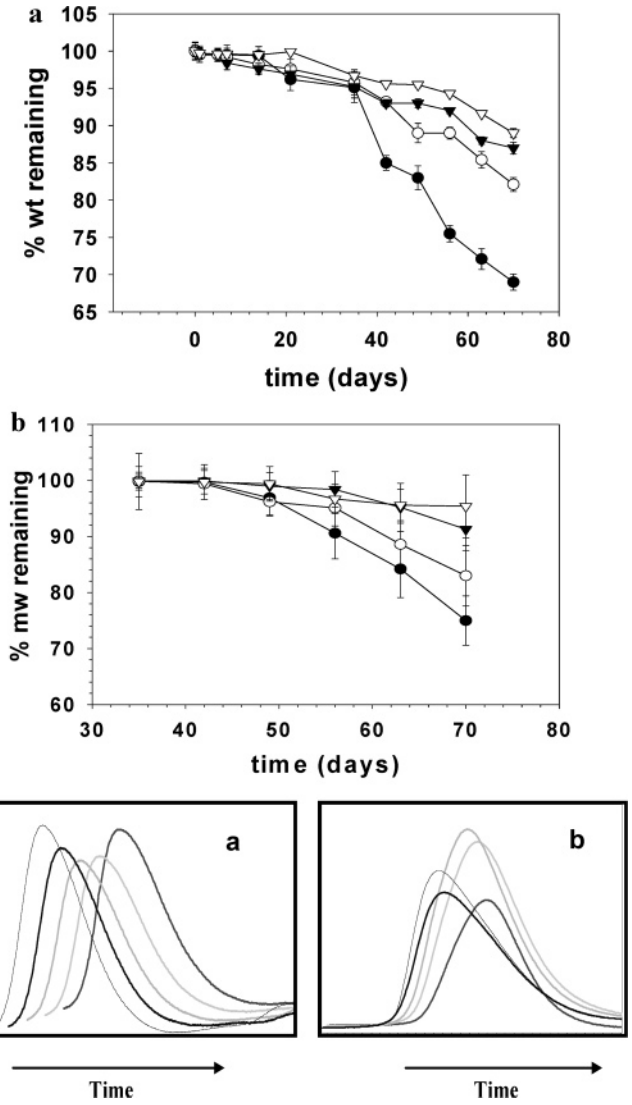

Figure 7. (a and b) Percent weight and molecular weight remaining as a function of time for (-●-) PLLA, (-○-) FluoroPLA5, (-▼-) FluoroPLA10, and (-▽-) FluoroPLA20 and GPC overlay chromatograms of (a) PLLA and (b) FluoroPLA20.

PLLA to copolymer. In the phase mode, nanophase separation is depicted by the white phases representative of the fluorinated domains which is increased as the degree of PFPE loading is increased. It is well documented that surface roughness can convey increased hydrophobicity of a material.[28,29] Average surface roughness (rms) values increased from 200 to 400 nm in the case of PLLA to FluoroPLA20. This observation offers a qualitative rationale for the increase in contact angles and changes in surface energies which is governed by the Young's equation relating interfacial tensions among the surface to the liquid and gas phase of a water droplet.[30] AFM micrographs showing phase and height images for PLLA and FluoroPLA20 and water drop profiles of PLLA and FluoroPLA films are displayed in Figure 5.

The complex dynamic viscosity data (cone−plate geometry) for PLLA, and FluoroPLA copolymers of similar molecular weight ranges, exhibited significant reduction in melt viscosity after incorporation of as low as 1 wt % PFPE as shown in Figure 6a. The flexible PFPE segments are likely acting as an internal plasticizer, allowing for improved flexibility in the PLLA polymer chains. The copolymers are melt-processable at a temperature (175 °C), significantly lower than that of the PLLA homopolymer (190−200 °C).

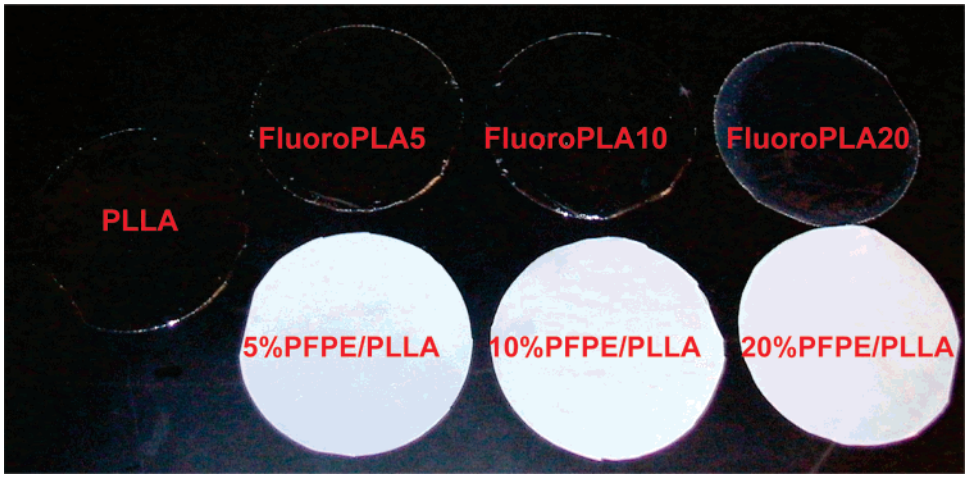

Figure 8. Photographs of spun cast films (from $CHCl_3$) of PLLA, 5−10 wt % FluoroPLA and the corresponding blends.

Incorporation of flexible elastomeric segments in a brittle matrix have been known to improve upon a biopolymers ductility.[25−27] FluoroPLA copolymers film strips from solvent casting and melt-spun fibers were tested using an Instron tensile tester. Tensile tests on thin strips of solution cast films and fibers of the copolymers reveal a stress−strain curve that is characteristic of a toughened plastic (Supporting Information Figure S1). Presence of PFPE segments (∼5 wt %) in the copolymer causes yielding of the specimen at constant yield stress and thereby enhances ultimate elongation of the fibers as shown in Figure 6b. At very low PFPE content (1 wt %) the effect is not very significant; whereas at very high PFPE content (10−20 wt %) the polymer molecular weight is significantly reduced and a weak brittle polymer is formed. Compared to the hard, brittle PLLA homopolymer, which has a higher modulus (initial slope of curve) and low ultimate strain (10−15%), the PLLA/PFPE copolymer containing 5 wt % PFPE can be elongated to over five times the elongation of PLLA before failure occurs. The tensile strength and modulus of the copolymers are slightly lower than that of the PLLA homopolymer. The variation of PFPE segment molecular weight in the 5 wt % copolymer further affects the ultimate strain.

Biodegradation studies have been performed in vitro to determine stability characteristics. The effects that PFPE has on PLLA's properties associated with hydrolysis and control of degradation can be determined by monitoring the polymer weight loss. Constant agitation for 60 days in phosphate buffered saline solution (PBS) at 37 °C in an incubator was performed to determine the rate of biodegradation. Parts a and b of Figure 7 show that PLLA homopolymer undergoes a substantial decrease in molecular weight and mass loss as compared to the FluoroPLA 5−20 copolymers. The effect of incorporating PFPE into PLLA lowers the rate of degradation or hydrolysis of PLLA in vitro depending upon the amount of PFPE incorporated. PLLA degrades at a faster rate in the PBS solution and hence % molecular weight remaining decreases significantly. The GPC overlay chromatograms (shown as inset of mass degradation in Figure 7b) show the curves for PLLA and FluoroPLA20 samples aged in PBS solution for 42 to 70 days. For PLLA homopolymers, the eluent curves of aged samples are uniformly shifted toward higher elution time. However, in the case of FluoroPLA20, the peaks of the curves for the aged samples are not distinctly separated, indicating nonuniformity and a lower degree of hydrolysis or degradation.

The use of fluorinated polyether oligomers for initiation of L-lactide monomer afforded the first FluoroPLA copolymer of its kind. Fluoropolyether segments impart optical clarity, improved ductility, reduced surface energy and water wettability, and excellent melt-processability with a minimum of fluorine incorporation. These novel polymers can be processed into fibers and films of desired properties for specific applications. Degradation of PLLA can be diminished significantly upon addition of PFPE segments. This allows one to tailor properties of PLLA at various environmental conditions (humidity, temperature, pH, etc.) for controlled biodegradation and permeability. Incorporation of fluorinated oligomers to PLLA increases the general use for PLLA in oil, water, and soil repellency. These materials have potential to replace petrochemical-based polymers in commodity areas such as plastics and textiles where properties can be tailored depending upon end use requirements.

Acknowledgment. We thank the U.S Department of Education for a GAANN Fellowship and an NSF SEAGEP fellowship to D.H., the National Science Foundation through the Center for Advanced Engineering Fibers and Films (NSF-ERC) and The Department of Commerce through the National Textile Center (NTC). We also thank Dr. Ivan Wlassics and Solvay Solexis, S.p.A. for their generous donation of Fomblins Z Dol materials and we thank Dr. Stephen Foulger and the Center for Optical Materials Science and Engineering Technologies (COMSET). D.W.S. is a Cottrell Scholar of the Research Corporation.

Supporting Information Available: Table giving surface energies of PLLA and PFPE/PLLA copolymers and figure showing stress−strain curves of PLLA, FluoroPLA 5, and 5 wt % PFPE/PLLA blend. This material is available free of charge via the Internet at http://pubs.acs.org.

References and Notes

(1) Dresselhaus, M. S.; Thomas, I. L. *Nature (London)* **2001**, *414*, 332−337.
(2) Ragauskas, A. J.; et al. *Science* **2006**, *311*, 484−489.
(3) Beach, E. D.; Boyd, R.; Uri, N. D. *Appl. Math. Model* **1996**, *20*, 388−398.
(4) Wool, R.; Sun. X. S. *Biobased Polymers and Composites*, 1st ed.; Elsevier Academic Press: Boston, MA 2005; pp 1−12.
(5) Gruber, P. R.; Hall, E. S.; Kolstad, J. J.; Iwen, M. L.; Benson, M. D.; Borchardt, R. L. US Patent 5,484,881, 1996.
(6) Ray, S. S.; Bousmina, M. *Prog. Mater. Sci.* **2005**, *50*, 962−1079.
(7) Albertsson, A.-C.; Varma, I. K. *Biomacromolecules* **2003**, *4*, 1466−1486.
(8) Lunt, J. *Polym. Degrad. Stab.* **1998**, *59*, 145−152.
(9) Deng, F.; Bisht, K. S.; Gross, R. A.; KaPLLAn, D. L. *Macromolecules* **1999**, *32*, 5159−5161.
(10) Edlund, U.; Kallrot, M.; Albertsson, A- C. J. *Am. Chem. Soc.* **2005**, *127*, 8865−8871.

(11) Abayasinghe, N. K.; Smith, Jr. D. W. *Macromolecules* **2003**, *36*, 9681−9683.
(12) Haynes, D.; Cureton, L.; Smith, Jr. D. W. *Prepr. Pap. (Am. Chem. Soc., Div. Polym. Chem.)* **2006**, *47*, 173−174.
(13) Anderson, K. S.; Lim, S. H.; Hillmyer, M. A. *J. Appl. Polym. Sci.* **2003**, *89*, 3757−3768.
(14) Noda, I.; Satowski, M. M.; Dowry, A.; Marcott. C. *Macromol. Biosci.* **2004**, *4*, 269−275.
(15) Vert, M.; Christel, P.; Chabot, F.; Leray, J. In *Macromolecular Biomaterials*; Hastings, G. W., Ducheyne, P., Eds.; CRC/Press Inc.: New York, 1984; p 119.
(16) Karis, T. E.; Marchon, B.; Hopper, D. A.; Siemens, R. L. *J. Fluorine Chem.* **2002**, *118*, 81−94.
(17) Bongiovanni, R.; et al. *J. Polym. Sci., Part A: Polym. Chem.* **2005**, *43*, 3588−3599.
(18) Shi, Z.; Holdcroft, S. *Macromolecules* **2004**, *37*, 2084−2089.
(19) Sanguineti, A.; Guarda, P. A.; Marchionni, G.; Ajroldi, G. *Polymer* **1995**, *36*, 3697−3703.
(20) Ameduri, B.; Boutevin, B. *Topics in Current Chemistry*; Springer: New York, 1997; Vol. 192, pp 168.
(21) Owens, D. K.; Wendt, J. *J. Appl. Polym. Sci.* **1969**, *13*, 1741−1747.
(22) Kaelble, D. H. *Surface Energy Criteria of Adhesion, Physical Chemistry of Adhesion*; Wiley-Interscience: New York, 1971; p 158.
(23) Biresaw, G.; Carriere, C. J. *J. Polym. Sci., Part B: Polym. Phys.* **2002**, *40*, 2248−2258.
(24) Kaelble, D. H.; Cirlin, E. H. *J. Polym. Sci., Part A*-2 **1971**, *9*, 363−368.
(25) Nagapudi, K.; et al. *Macromolecules* **2005**, *38*, 345−354.
(26) Younes, H. M.; Bravo-Grimaldo, E.; Amsden, B. *Biomaterials* **2004**, *25*, 5261−5269.
(27) Yang, J.; Webb, A.; Pickerill, S.; Hageman, G.; Ameer, G. *Biomaterials* **2006**, *27*, 1889−1898.
(28) Cassie, A. B. D.; Baxter, S. *Trans. Faraday Soc.* **1944**, *40*, 546.
(29) Wenzel, R. N. *Ind. Eng. Chem.* **1936**, *28*, 988.
(30) Young, T. *Philos. Trans. R. Soc.* **1805**, *95*, 65.

MA0712192